Reviewer #1: Christopher Horvat

CH: *This manuscript uses shipboard camera images taken over a transect of the Antarctic MIZ to describe the pancake floe size distribution in that region. The manuscript is sets out its goals, and accomplishes them concisely and straightforwardly, and so I recommend its publication in short order: this information is valuable and interesting to those who are trying to evaluate and understand sea ice models that incorporate the physics of small floes. I do have some relatively minor issues, mainly related to presentation and data processing, that I would like to see improved upon before publication. These are listed below - if any comments are unclear please contact me with questions.*

AA: We thank the referee for his very positive comments. Below we provide answers to all the comments.

CH: *Page 1 Line 10 - I believe the paper of yours truly you mean to cite is H+T 2015, as that is the model paper.*

AA: We agree that H+T 2015 is the better reference and thus we added it in the revised manuscript.

CH: *Page 1 Line 11 - While it is true early results show the importance of the FSD at the edge, only floe breaking by waves and floe melting has been put in models, so it isn't true that this is the place where floes are most important as we don't have a handle on their evolution deeper into the pack.*

AA: We have changed the statement.

CH: *Page 1 Line 12 - Please cite either Steele, 1992, or Horvat et al, 2016 when making the statement about floe melting.*

AA: Reference to Steele 1992 has been added.

CH: *Page 1 Line 13 - I would delete "formed ... currents" as you also mention the importance of waves for pancake formation, and winds and currents can significantly alter the formation mechanism of sea ice in the MIZ.*

AA: The phrase has been deleted.

CH: *Page 1 Line 15 - change "exhibits" to "resembles" as you argue below the inapplicability of fractal scaling.*

AA: The change has been made.

CH: *Page 2 Line 3 - add citations to Herman 2014, 2017 here as it is important for readers to know there is really not much evidence of a multi-decadal power law.*

AA: The section has been rewritten and clarified to provide a better overview of previous literature, including the papers by Herman (noting that Herman 2014 should be Herman 2010).

CH: *Page 2 Line 5 - Both papers cited here really argue *against* the adoption of FSD power laws, not for them!*

AA: We agree with the reviewer. We rephrased this section and added a reference to Herman et al. 2017 to make this statement clearer.

CH: *Page 2 Line 16 - "the *Antarctic* sea ice annual mass budget".*

AA: Added.

CH: *Page 2 Line 18 - I'm not sure the statement about pancakes being more common is supported by the Roach et al paper as it is a point measurement.*

AA: We changed "common" to "frequent than in the past". We added a reference to Wadhams et al. (2018) where such a claim is made explicitly. We have kept the reference Roach et al. (2018), which specifically

focusses on pancakes and where this statement, supported by a number of references, appears at the end of the first paragraph of the Introduction.

CH: *Page 3 Fig 1 - I would like to see this visualization improved, and the caption more descriptive. For example, it isn't clear that (a-b) and (c) are on different axes immediately, and isn't mentioned that (c) is the cutout in (a-b). Also, are the measurements you are making the dark line in (c)? Could you add the green dash to (a-b) as well?*

AA: We now indicate explicitly in the caption that (c) is a subdomain of (a) and (b) where it is indicated by a white frame. We also added that the black part of the track in (c) indicates where cameras were operational and measurements undertaken. The green mark in (a) and (b) is superfluous as the area of interest is already framed in white and would clutter the figure.

CH: *Page 3 Line 8 - explain what you mean about statistical independence.*

AA: We now added that this means that the sampled area in two subsequent images is different (i.e. no overlap) thus all the floes are only measured once.

CH: *Page 3 Line 8-15 - generally, please explain the operation used to compute the pancakes as this is very important information for reproducing or building from this work.*

AA: A brief description has been added. The procedure is fairly standard and only uses a series of MatLab built-in functions. We point out that development of the algorithm is not the focus of this communication. Details are now given in the supplementary material. The algorithm and data are available upon request.

CH: *Page 4 Line 5 - please explain why one might decline an image.*

AA: Visual inspection of the processed images quickly reveals images to be disregarded, e.g. when the reconstructed floes didn't match the greyscale image in a macroscopic way. In general, images where discarded when a large number of separated floes were merged together (i.e. only one identified floe by the algorithm, we define such instance artificial welding) or when single floes were split in a number of smaller floes by the algorithm.

CH: *Page 4 Line 8 you explain why AMSR might *overestimate* concentration, but for many points along the track it underestimates concentration - explain.*

AA: AMSR2 averages two daily swaths. During the measurements the intense storm conditions induced an ice drift of the order of 100km Eastward. In this circumstance it is likely than one or even both swaths occurred over open water thus leading to underestimation the instantaneous observed ice concentration (e.g. at the beginning of the recording). A comment has been added in the revised manuscript.

CH: *Line 18 - "prone to error" - what kind of error? why?*

AA: The extent of these floes is only few pixels. Higher resolution (i.e. px/m) would be required to reliably reconstruct the shape of these floes. A comment has been added in the revised manuscript.

CH: *Line 19 - why were the welded floes excluded? Isn't this the process by which these pancakes are said to form? What criteria is used to pick floes to exclude, and how does this affect the tail of your distributions in Fig 3?*

AA: Only artificially welded floes are excluded, i.e. those that are made by two separated floes but the algorithm returns as one single floe. Real welded floes are still included. A comment has been added in the revised manuscript to clarify the concept of artificially welded floes.

CH: *Line 20 - area = 1.55 km^2 - I thought the swath was 28 m, which would mean you traveled 55 km into the ice, not close to 100 km.*

AA: The swath itself would be 55km by 28m but this is distributed over a ship track of 100km. Two subsequent images are not contiguous in space to avoid overlap and guarantee statistic independence of the sampled floes. A comment has been added in the revised manuscript.

CH: *Page 5 Figure 3 - You have extra space in this figure - could you please also plot the area weighted FSD rather than the number size distribution? The area size distribution is what appears in the Roach et al model and so would be good to see. You can estimate how much spread there is in (a) by taking D_1 and adding white noise to it and calling that D_2, then re-sorting in the instances D_2 > D_1. the magnitude of the white noise that is required to get the fit line would tell you how much error there is in assuming a circle.*

AA: Figure 3 has been revised, with additional subplots and insets. The area distribution is presented in 3b (cumulative) and 3e (pdf, previously in 3b).

In response to this comment we show the empirical distribution of the D2/D1 ratio in figure 3a which provides information on the scatter of D2/D1. To better describe the shape of the floes we added the scatter plot of the circularity as a function of the diameter (figure 3d in the revised manuscript). We believe this to be a better way to describe the shape of the floes and is more commonly used than the method suggested by the referee.

CH: *Line 2 - why the mode = peak probability? Why not the mean, and could you report the "roundness" of the floes?*

AA: The mode is extracted from the floe area distribution (i.e. the FSD expressed in terms of area instead of floe number as shown in Fig 3b and 3e in the revised manuscript). Mean and median are also reported in the revised manuscript noting that in terms of area distribution mode, median and mean are all about 3.1m.

CH: *Line 4 - That the probability of exceedence hides the fact of a non-power-law distribution is extremely interesting and while some have discussed this in model papers, to my knowledge this is the first time this has been evidenced *on purpose* in an observational paper. I would like to see this highlighted!*

AA: We added a statement to highlight this concept in the conclusions.

CH: *Line 12 - I don't think you can say that there is a different physical mechanism to make larger floes as you only have a point observation of welding.*

AA: Visual inspection of a large number of the images reveals that a considerable number of the larger floes are formed by smaller floes welded together. The line of welding is clearly visible from the images (see video in the supplementary material). These relatively large floes contribute the most in shaping the tail of the FSD. It is very likely then that welding process (for which importance has been shown by Roach et al., 2018), is the physical process that mostly affects the FSD in this regime, but this conjecture has to be further verified. The statement in the manuscript has been modified.

CH: *Line 25 - The point about dropping a priori assumptions is good, I would add that using a KDE is in some ways equivalent to fitting distributions to power laws: both are not derived from first principles and so both give little insight into the actual physics governing the distribution.*

AA: We made no change in response to this comment, as the point we were trying to make is that using a KDE involves no assumptions about the shape of the FSD.

Reviewer #2: Anonymous

R2A: *The authors acquired images of pancake ice floes from a ship-based camera on July 4, 2017, in the Antarctic marginal ice zone at about 30E, 62S. An automatic algorithm identified pancake ice floes in the images, whose size distribution was then plotted. They found three size regimes: diameters 0.25 to 2.3 meters, 2.3 to 4 meters, and 4 to 10 meters (see Figures 3b and 3d). They conjecture that the small regime is driven by the growth of pancakes from frazil ice, and the large regime is driven by the welding together of pancakes.*

AA: We thank the reviewer for his/her comments and constructive criticisms. The manuscript has been modified to address the comments and detailed answer to each of the comments is given below.

R2A: *This paper is basically a report of data analysis. The conjectures regarding the small and large floe regimes are just that – conjectures – without supporting evidence. I have questions about the analysis, detailed below, as well as other comments. In my opinion, this paper needs major revisions.*

AA: We agree with the reviewer that this brief communication reports data analysis, however, this overlooks that the present work increases knowledge on the subject as it provides the first quantitative measurements of pancake ice floes in the Antarctic marginal ice zone, as well as the first assessment of the pancake ice floe distributions (for area and diameter), based on a very large number of floes (results are statistically significant). We also compare with distributions traditionally proposed for sea ice and assess floe shape. Moreover, we point out that our conjectures (as we ourselves define them) need to be verified, and that they are based on previous work of Roach et al. (2018), in which these mechanisms are studied but without discussing the pancake ice floe size distribution and shape.

R2A: *Page 1, lines 9-10. The floe size distribution (FSD) was first integrated into a sea-ice model by Zhang et al in 2015 and 2016.*

AA: We added references to Zhang et al. (2015,2016).

R2A: *Page 1, lines 12-15. The authors imply that there is not much "field data" available on floe sizes. I assume this refers to in-situ data such as that acquired from a ship in the ice. But there is plenty of remote sensing data, and it's not clear to me that field data is any better than remote sensing data, so the lack of field data does not seem like a shortcoming. The only advantage I can see to field data is the higher spatial resolution – in this case, the ability to identify floes as small as 0.25 m in diameter. But this advantage is not mentioned by the authors. Perhaps one of the values of this study is that it identifies floes that are smaller than in any other study. The fact that it consists of data collected in the field is not in itself a selling point, in my opinion.*

AA: We understand the possible misunderstanding with the use of "field data". We have clarified the different role played by in situ observations of smaller floes in the Southern Ocean and that there are no previous observations of pancake ice in this region, as their small scale makes them difficult to resolves from space.

R2A: *Page 2, lines 2-4. This is really an oversimplification. It is certainly true that observations do not support a unique scaling exponent of the FSD – that was the subject of an entire paper (Stern et al 2018) which is cited by the authors later but not here. Only some of the 18 studies examined in that paper report "two distinct scaling exponents". The authors imply that those exponents are given by Toyota et al 2011, but other studies have found different exponents over different ranges, and some have reported that a single exponent characterizes the FSD.*

AA: We rephrased the sentence to clarify this concept, also using Stern et al. (2018) as the main reference. We note that no previous works refer to pancakes, and we have further emphasized this as a novelty of our study.

R2A: *Page 2, lines 5-6. "The validity of power law scaling has not been demonstrated yet and its adoption is mostly justified by the wide range of floes diameters". Actually the validity of power-law scaling has been demonstrated in some cases, and I have never seen a paper that claims that power-law scaling is justified by the wide range of floe diameters. The papers cited by the authors don't make that claim.*

AA: We thank the reviewer for helping us to clarify this point. We rephrased the section to emphasise that the alpha = 2 exponent is not universal, and the power law behaviour is not verified in all the cases reported in the literature. We also added references to Horvat & Tziperman (2017) and Herman et al. (2017) to strengthen the statement.

R2A: *Page 2, lines 6-7. "Scaling parameters are typically estimated on the log-log plane with a least square fit" – it would be good to note that such a procedure leads to a biased estimate of the scaling parameter.*

AA: This note has been added.

R2A: *Page 2, line 12. "Existing observations do not provide quantitative descriptions of the floe size distribution for pancake ice floes", but line 19 says "Shen and Ackley (1991) reported pancake floe sizes..." so doesn't that contradict line 12?*

AA: We have clarified that Shen & Ackley report a characteristic diameter only, i.e. not the floe size distribution as done in this work.

R2A: *Page 2, line 26. "To our knowledge, the pancake floe size distribution has yet to be characterized." Take a look at: Parmiggiani, Moctezuma-Flores, and Guerrieri, Identifying pancake ice and computing pancake size distribution in aerial photographs, Proc. SPIE 10422, Remote Sensing of the Ocean, Sea Ice, Coastal Waters, and Large Water Regions 2017, 104220K (13 October 2017); doi: 10.1117/12.2277537*

AA:. We rephrased the statement to include this reference. However, we note that the paper only focusses on development of a processing scheme for pancake floe detection. Only one image is analysed and results are reported in terms of pixels (no dimensions are reported), so the paper does not provide a quantitative characterisation of the pancake ice distribution, as we have done in this study over a larger region.

R2A: *Section 2, Sea ice image acquisition. All good, nice work. I do have one comment: page 3 line 14 says that morphological image processing was used "to improve the shape of the pancake floes." I don't think "improve" is the right word! How about "to smooth"?*

AA: Morphological operations are indeed used to improve or enhance the identification of the floes. We made no change in response to this comment in the manuscript but, to clarify the processing technique, we added a full list of morphological operations we adopted in the new supplementary material.

R2A: *Page 4, lines 15-17. There is more than one way to define the floe diameter D. The first study of the FSD, Rothrock and Thorndike 1984, used the mean caliper diameter.*

AA: A note that the caliper diameter can be used as the characteristic dimension has been added.

R2A: *Page 5, line 5. "a power law N(D) proportional to D^-alpha as a benchmark and using the maximum likelihood method". Here, N(D) is the cumulative distribution function (CDF), but the maximum likelihood method yields the best-fitting exponent of the probability density function (PDF), not the CDF. If the authors used the maximum likelihood method to obtain the best-fitting exponent of the PDF (call it -beta), then they would have had to convert it to the exponent of the CDF (via -alpha = -beta + 1). Did they do this?*

AA: We rephrased the statement to make clear that we used the procedure described in Stern et al. (2018), which is based on Clauset et al. (2009).

R2A: *Page 5, lines 6-8. The authors note that the range of floe sizes for the large regime (4 to 10 meters) spans less than a factor of 10, and therefore "the estimation of the scaling exponent for D > 4 m is rigorously not applicable". Well, the same is true for the small floe regime (0.25 to 2.3 meters) – it spans less than a factor of 10, so apparently the estimation of the scaling exponent for D < 2.3 m is rigorously not applicable either. Doesn't that destroy the basis of the floe size analysis here?*

AA: We rephrased to indicate that also in the small floe regime the range is less than a decade. However, this would only `destroy' our analysis and findings if we were advocating that the distribution is a power law, when, in fact, we emphasise that it is not a power law.

R2A: *Page 5, lines 12-13. "the steeper slope indicates that their size is governed by different underlying physical mechanisms." Or by the finite size effect, in which larger floes are under-observed because the finite size of the images makes it less likely to see larger floes in their entirety. This has been described in the literature. Can the finite size effect be ruled out here?*

AA: Indeed, finite size effects can be ruled out, as the floes for which the change in slope occurs (~4 m) are considerably smaller than the image footprint (~28 m x 28 m). Even the largest floe recorded (~10 m) is less than 2 times than the dimension of the image. Therefore, we conjecture that the clipping at ~10 m is due to a physical mechanism.

R2A: *Page 5, Figure 3. It looks to me like Figure 3b (the area distribution, a(D)) is not compatible with Figure 3d (the PDF, n(D)). In 3b, the area distribution increases as D increases, from D=0.2 to D=3. In that range, alpha_S = 1.1 so alpha_S + 1 = 2.1 so the PDF n(D) scales like D^-2.1. The area of a floe scales like D^2. So the area distribution a(D) should scale like D^(-2.1 + 2) = D^-0.1. That means the area distribution should DECREASE as D increases from D=0.2 to D=3. But Figure 3b shows a(D) increasing as D increases over that range. Is there something wrong with the plots, or with my analysis?*

AA: The reviewer's analysis is correct and we understand that the estimation of the coefficients and their application to the area distribution require further explanation. We note that the value of the exponent depends on the range over which computations are made, and, in this regard, the value 2.3 m is arbitrary. Since the CDF is concave-down, by reducing the range over which the exponent is estimated a lower slope can be obtained (eventually the exponent might drop below alpha_S = 1, thus leading to an increasing area distribution). Moreover, the discrepancy between a power law behaviour for the number distribution and the measured area distribution further demonstrates that the underlying number distribution is, in fact, not a power law (as also indicated by the goodness of fit test). We now explicitly point out this apparent discrepancy: *"We also note that an increasing alpha(D) in the small-floe regime (see Figs. 3e) is inconsistent with a power law with alpha_S ≥ 1 and, thus, the area distribution confirms that the underlying number distribution is not a power law."*

R2A: *Page 5, line 13. "the majority of the large floes are composed of two or more welded, pancakes." Does this explain some of the scatter in Figure 3a, in which a welded pair of pancakes would have a large major axis (D1) compared to minor axis (D2)?*

AA: We can't say with certainty if the scatter is due to welding. However, we note that the scatter is fairly homogeneous across all diameters in the range, whereas welding dominates for large pancakes only. This information was based on visual observations and we now provide a sample video of the acquired images as supplementary material to help the reader.

R2A: *Page 6, lines 16-18. It's commendable that the authors applied a goodness-of-fit test, and that they admit that neither the small nor the large floe size regime follows a power law distribution according to that test. This result is actually not too surprising, given the very small size ranges over which the power laws were fit.*

AA: We point out that the choice of fitting and testing a power law derives from the traditional sea-ice approach, well knowing that the range of diameters is small. A comment has been added in the revised manuscript.

R2A: *Page 6, lines 19-20. "N(D) possesses a slightly concave-down curvature across all the diameter ranges (in a log-log plane)". This phenomenon has been noted, or can be seen, in many previous studies, such as Rothrock and Thorndike 1984, Toyota et al 2016, Wang et al 2016 (JGR), and Stern et al 2018, where it is discussed at length.*

AA: As pointed out by Stern et al. (2018), this behaviour relates to the fact that the underlying distribution might be a truncated power law. We added a note on this in the revised manuscript.

R2A: *Page 6, lines 25-29. This is a good paragraph, with entirely appropriate conclusions. Please note that it applies only to the pancake floes analyzed here, and not to the FSD in general.*

AA: We thank the reviewer for the positive comment and we added a note, as suggested.

R2A: *Page 6, Conclusions. This section simply re-hashes the division of the FSD into three regimes. It claims that the small and large floe size regimes are "qualitatively close to power law scalings", but that is a very dubious characterization, especially for the large floe regime, where the range of floe sizes spans less than half an order of magnitude: log(10.8/4) < 1/2.*

AA: We rephrased and removed any reference to power-law behaviour. In the revised manuscript we write: *"Two different behaviours are observed for smaller and larger pancakes on a log-log plane. The small-floe*

regime (D < 2.3 m), in which it is conjectured that pancakes are experiencing thermodynamic growth, is characterised by a mild negative slope (in terms of the floe number exceedance and probability density function), while the large-floe regime, in which floes are typically formed by welding (detected from visual analysis), is characterised by a much steeper slope noting that neither of the two regime conforms to a power law scaling."

***R2A**: The authors do not give a mechanism by which the FSD of the small floe regime comes to be qualitatively close to power-law scaling. They only state that the "pancakes are experiencing thermodynamic growth". How does that lead to power-law scaling?*

AA: Based on observations by Roach et al. (2018), we hypothesise that thermodynamic growth is a potential mechanism leading to the observed FSD in the small-floe regime. We rephrased the relevant section to clarify that this statement is fairly speculative and, in the spirit of a brief communication, only serves to stimulate further research. We certainly do not claim that this mechanism leads to a power law.

***R2A:** For the large floe regime, they write that "floes are typically formed by welding". That's a mechanism that can be easily simulated in a numerical experiment, and the results compared to the actual (observed) distribution. I have taken the liberty of conducting such an experiment, which did not take very much time to code up – see the attached figure. I started with 20,000 floes whose sizes were distributed according to a power law with exponent -2 and ranging from 0.25 to 3.0 meters in diameter. See the black curve in the attached figure. I then simulated a welding process in which two randomly chosen floes were welded together according to D_new = sqrt(D1^2 + D2^2) where D1 and D2 are the diameters of the floes to be welded, and D_new is the diameter of the welded floe. The floes with D1 and D2 are removed from the distribution, D_new is added to the distribution, and the process is repeated 5000 times, leaving 15,000 floes. The resulting distribution is shown by the red curve. The procedure is repeated again (5000 times), leaving 10,000 floes (green curve), and again (5000 times), leaving 5000 floes (blue curve). The blue curve has some qualitative similarities to Figure 3d. This is not a very sophisticated simulation, and I am not suggesting that the authors need to do something like this, but it does demonstrate the potential for mimicking certain processes. Of course a physical model would be better, but that is probably beyond the scope of the present study*

AA: The statements that large floes are formed by welding derive by visual analysis of the acquired images and observations made from the ship deck. We have added footage as supplementary material to support the statements. The reviewer's suggestion and proposed simulations are certainly interesting, and we also agree that a detailed investigation of this kind would go far beyond the scope of the present brief communication. We would like to emphasize the main aim of the work which is to report the first quantitative observations on the pancake ice floe size distribution and to stimulate further research.

In the revised manuscript we note that these results reflect observations collected under storm conditions (see Fig. 1) and thus they may not be applicable to all the sea-ice states. We indicate that simultaneous measurements of waves, floe size and heat fluxes under a number of different conditions are indeed needed to verify the conjecture that different physical mechanisms are responsible for the peculiar shape of the pancake ice floe size distribution with the intention of stimulating further research.

Brief communication: Pancake ice floe size distribution during the winter expansion of the Antarctic marginal ice zone

Alberto Alberello[1,*], Miguel Onorato[2,3], Luke Bennetts[4], Marcello Vichi[5,6], Clare Eayrs[7], Keith MacHutchon[8], and Alessandro Toffoli[1]

[1]Department of Infrastructure Engineering, The University of Melbourne, Parkville, VIC 3010, Australia.
[2]Dipartimento di Fisica, Università di Torino, Torino, 10125, Italy.
[3]INFN, Sezione di Torino, Torino, 10125, Italy.
[4]School of Mathematical Sciences, University of Adelaide, Adelaide, SA 5005, Australia
[5]Department of Oceanography, University of Cape Town, Rondenbosch, 7701, South Africa.
[6]Marine Research Institute, University of Cape Town, Rondenbosch, 7701, South Africa.
[7]Center for Global Sea Level Change, New York University Abu Dhabi, Abu Dhabi, United Arab Emirates.
[8]Department of Civil Engineering, University of Cape Town, Rondenbosch, 7701, South Africa.
[*]now at: School of Mathematical Sciences, University of Adelaide, Adelaide, SA 5005, Australia

Correspondence: Alberto Alberello (alberto.alberello@outlook.com)

Abstract.

The size distribution of pancake ice floes is calculated from images acquired during a voyage to the Antarctic marginal ice zone in the winter expansion season. Results show that 50 % of the sea ice area is made up by floes with diameters 2.3–4 m. The floe size distribution shows two distinct slopes on either side of the 2.3–4 m range. ~~It~~ Following a relevant recent study, it is conjectured that growth of pancakes from frazil forms the distribution of small floes ($D < 2.3$ m), and welding of pancakes forms the distribution of large floes ($D > 4$ m).

1 Introduction

Prognostic floe size distributions are being integrated into the next generation of large-scale sea ice models ~~(Horvat and Tziperman, 2017; B~~ (Horvat and Tziperman, 2015; Zhang et al., 2015, 2016; Bennetts et al., 2017; Roach et al., 2018a). Early results show that the floe size distribution ~~has the greatest impacts on~~ affects ice concentration and volume close to the ice edge, in the marginal ice zone, where ocean waves regulate floe sizes and floes are generally the smallest, meaning they are prone to melting in warmer seasons (Steele, 1992). However, at present the only field data available to validate and improve the models are empirical distributions derived for pack ice ~~formed from ice breakup due to winds, waves and currents, and~~ spanning several orders of magnitude (from few meters to tens of kilometres; e.g. Toyota et al., 2016) and none resolve floes below the meter scale.

Break up of pack ice often ~~exhibits~~ resembles a fractal behaviour ~~similarly~~ similar to many brittle materials (Gherardi and Lagomarsino, 2015). It has been argued that exceedance probability of the characteristic floe size, D, expressed as number of

floes, follows a power law $N(D) \propto D^{-\alpha}$, where the scaling exponent is $\alpha = 2$ if a fractal behaviour is assumed (Rothrock and Thorndike, 1984). ~~Observations, from both the Arctic and Antarctic, do not support the existence of a unique scaling exponent (Steer et al., 2008; Toyota et al., 2011), with two distinct scaling exponents of the exceedance probability reported. For small floes (tens of metres and below) the exponent is $\alpha = 1.03–1.52$, while~~

Most of the previous observations of the floe size distribution in the marginal ice zone (noting that no observations are in pancake ice conditions) conform to a truncated power law (Stern et al., 2018), with the α value varying among studies depending on season, distance from the ice edge and range of measured diameters. Some of the measurements in the Antarctic support a split power law, with a mild slope for smaller floes and a steeper one for larger floes~~$\alpha = 3.40–7.59$ (Toyota et al., 2011)~~, suggesting that different mechanisms govern the distributions for small and large floes (Steer et al., 2008; Toyota et al., 2011).

The validity of the power law scaling has not been demonstrated yet (Horvat and Tziperman, 2017) and its adoption is mostly justified by the wide range of floes diameters ~~(Horvat and Tziperman, 2017; Stern et al., 2018)~~(Herman et al., 2017). Scaling parameters are typically estimated on the log-log plane with a least square fit, which leads to biased estimates of α, and, as noted by Stern et al. (2018), without rigorous goodness-of-fit tests. In comparison, Herman et al. (2017) examined the size distribution of floes under the action of waves in controlled laboratory experiments, by analysing the probability density function $n(D)$, which revealed a fractal response due to an arbitrary strain (a power law) superimposed to a Gaussian break up process induced by the waves. The interplay of these mechanisms is hidden in the floe number exceedance probability.

Existing observations do not provide quantitative descriptions of the floe size distribution for pancake ice floes, which form from frazil ice under the continuous action of waves and thermodynamic freezing processes (Shen et al., 2004; Roach et al., 2018b). This is important, for example, during the Antarctic winter sea ice expansion, when hundreds of kilometres of ice cover around the Antarctic continent is composed of pancake floes of roughly circular shape and characteristic diameters 0.3–3 m (Worby et al., 2008). Pancake floes represent most of the Antarctic sea ice annual mass budget (Wadhams et al., 2018). Moreover, in the Arctic, pancakes are becoming more ~~common~~ frequent than in the past due to the increased wave intensity associated with the ice retreat ~~(Roach et al., 2018b).~~ (Wadhams et al., 2018; Roach et al., 2018b).

Shen and Ackley (1991) reported pancake floe sizes from aerial observations collected during the Winter Weddell Sea Project (July 1986), showing that pancake sizes increase with distance from the ice edge, from 0.1 m in the first 50 km up to ≈ 1 m within 150 km from the edge (but without investigating the floe size distribution). They attributed this to the dissipation of wave energy with distance into the ice-covered ocean, and proposed a relationship between wave characteristics, mechanical ice properties and pancake size (Shen et al., 2004). More recently, Roach et al. (2018b) used camera images acquired from SWIFT buoys deployed in the Beaufort Sea (Sea State cruise, October–November 2015) to quantify the lateral growth of pancakes and their welding. ~~The high~~ A correlation between wave properties and the size of relatively small pancakes (up to 0.35 m) was confirmed.

To our knowledge, the pancake floe size distribution has yet to be characterised, noting that although Parmiggiani et al. (2017) developed an algorithm for pancake floes detection, they did not provide quantitative indication on the shape and size of the

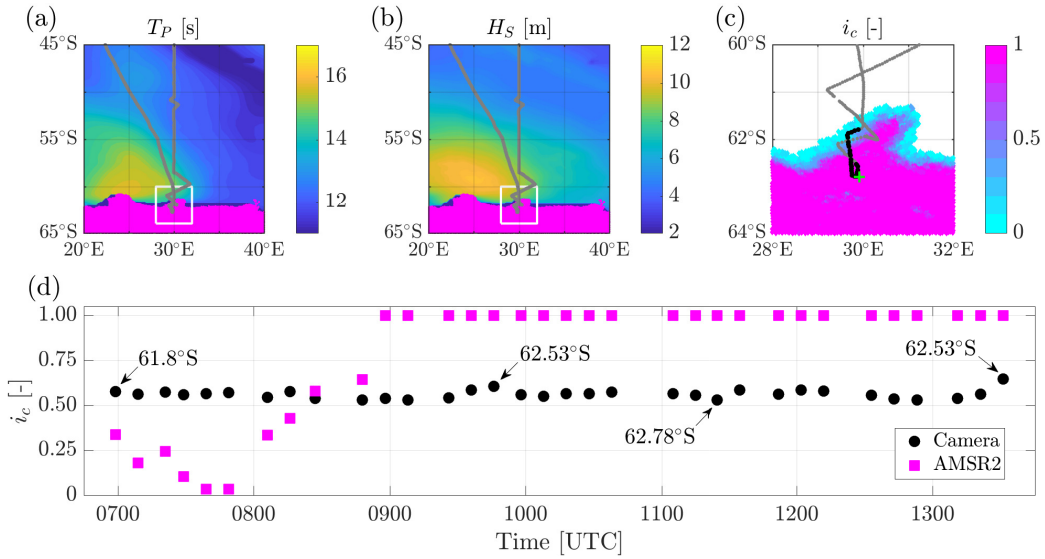

Figure 1. Environmental condition during on the 4th of July 2017 (local time UTC+2). Peak wave period (a) and significant wave height (b) are sourced from ECMWF ERA-Interim reanalysis. The magenta area denotes ice and grey dots show the ship track. In (c), which is the subdomain indicated by a white frame in (a) and (b), ice concentration is sourced from AMSR2 satellite with a 3.125 km resolution (Beitsch et al., 2014). The black dots denotes the position during which cameras were operational and measurements undertaken. The green cross the location of deployment of a wave buoy. In (d), pancake floe concentration reconstructed from the camera images is shown as black dots, and total ice concentration obtained from AMSR2 satellite at the location closest to the measurements is shown as magenta squares.

floes. Here, a new set of images from the Antarctic marginal ice zone are used to measure the shape of individual pancakes and to infer their size distribution.

2 Sea ice image acquisition

At approximately 07:00 UTC on the 4th of July 2017, the icebreaker S.A. Agulhas II entered the marginal ice zone between 61° and 63° South and approximately 30° East during an intense storm (see Fig. 1a,b for the ship track and a snapshot of peak wave period and significant wave height as sourced from ECMWF ERA-Interim reanalysis, Dee et al. 2011). A buoy was deployed in the marginal ice zone ≈ 100 km from the ice edge (green mark in Fig. 1c). At the time of deployment, the significant wave height was 5.5 m, with maximum individual wave height of 12.3 m. The dominant wave period was 15 s.

~~Environmental condition during on the 4th of July 2017 (local time UTC+2). Peak wave period (a) and significant wave height (b) are sourced from ECMWF ERA-Interim reanalysis. The magenta area denotes ice and grey dots show the ship track. In (c), ice concentration is sourced from AMSR2 satellite with a 3.125 km resolution (Beitsch et al., 2014). The black dots denotes the position during which cameras were operational and the green cross the location of deployment of a wave buoy.~~

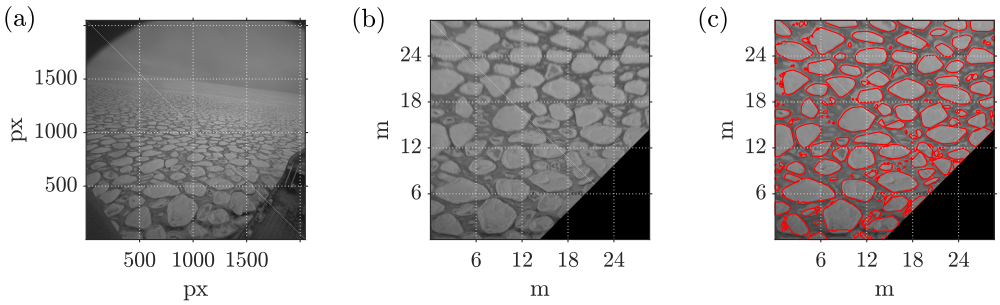

Figure 2. Sample acquired image (a), rectified and calibrated image (b) and detected pancakes (c).

~~In (d), pancake floe concentration reconstructed from the camera images is shown as black dots, and total ice concentration obtained from AMSR2 satellite at the location closest to the measurements is shown as magenta squares.~~

A system of two GigE monochrome industrial CMOS cameras with a 2/3 ~~inches~~ inch sensor was installed on the monkey bridge of the icebreaker to monitor the ocean surface. The cameras were equipped with 5 mm C mount lenses (maximum aperture $f/1.8$) to provide a field of view of approximately 90°. The cameras were installed at an elevation of ≈ 34 m from the waterline and with their axes inclined at 20° with respect to the horizon. The system was operated by a laptop computer. Images were recorded with resolution of 2448×2048 pixels and a sampling rate of 2 Hz during daylight on the 4th of July (from 07:00 to 13:30 UTC).

An automatic algorithm was developed using the MatLab Image Processing Toolbox (Kong and Rosenfeld, 1996) to extract sea ice metrics from the recorded images (see Fig. 2a for an example). To ensure statistical independence of the data set (i.e. to avoid sampling the same floe twice), only one camera and one image every 10 s was selected for processing (this interval guarantees no overlap between consecutive images). Images were rectified to correct for camera distortion and to project them on a common horizontal plane. A pixel to meter conversion was applied by imposing camera-dependent calibration coefficients. The resulting field of view is 28 m×28 m and resolution 29 px/m (see Fig. 2b). The image was processed to eliminate the vessel from the field of view, adjust the image contrast, and convert the grey scales into a binary map based on a user selected threshold. The mapping isolates the solid ice shapes from background water or frazil ice. The binary images, however, are noisy and require refining based on morphological image processes to improve the shape of the pancakes floes ~~.~~ (i.e. erosion, filling and expansion). Threshold selection and morphological operations are optimised to detect pancake floes only and exclude interstitial frazil ice. ~~The~~ (The optimisation is performed for the specific light and ice condition using this particular camera setup.) The resulting separated floes are shown in Fig. 2c. Post-processed images were visually inspected for quality control, and $\approx 5\%$ of the images were discarded due to unsatisfactory reconstruction of the pancakes. Macroscopic differences between the acquired image and the reconstructed floes were noted, e.g. multiple floes were detected as one (artificial welding) or individual floes were divided into multiple floes by the automatic algorithm.

Identification of individual pancakes allows estimation of the individual floe areas ~~A~~S. An overall ice concentration (i_c, Fig. 1d) can be computed as the ratio of the area covered by pancake floes to the total surface in the field of view. A representa-

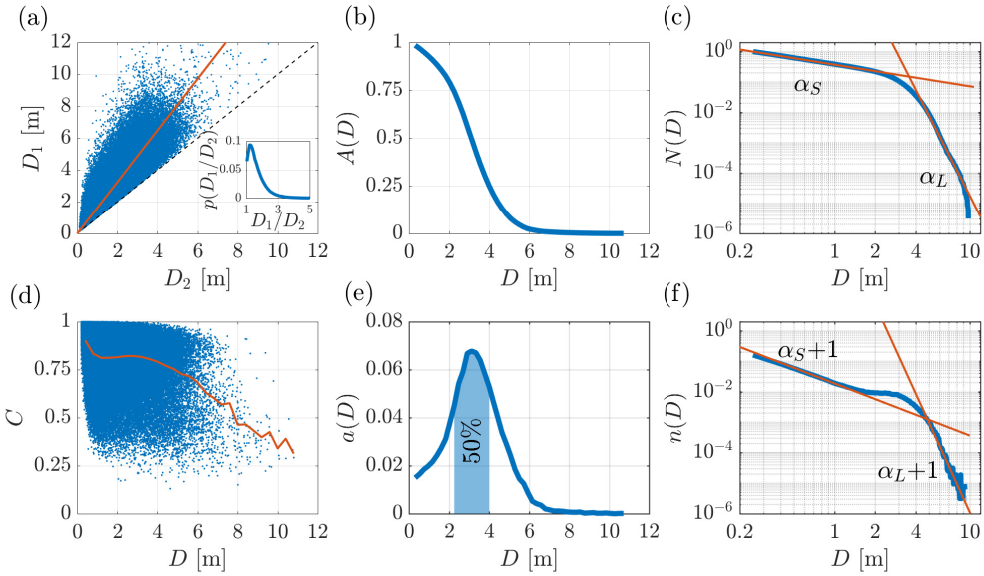

Figure 3. In (a), scatter plot of the major and minor axis of the pancake floe with the linear fit (solid orange line), the inset shows the probability density function of D_1/D_2. In (d), scatter plot of the circularity of the floes against the equivalent diameter and the average value (solid orange line). In (b), ice area distribution as a function of the floe diameter expressed as exceedance probability. In (e), ice area distribution as a function of the floe diameter expressed as probability density function. In (c), floe number exceedance probability $N(D)$ as a function of the floe diameter with two power law (solid orange lines) fitted for small ($D < 2.3$ m) and large floes ($D > 4$ m) respectively. In (f), floe number probability density function $n(D)$ as a function of the floe diameter with two power law (solid orange lines) fitted for small ($D < 2.3$ m) and large floes ($D > 4$ m) respectively.

tive concentration was estimated every 60 consecutive images (i.e. 10 min time window), which is equivalent to a sampled area of 0.047 km^2. Pancake concentration was consistently $\approx 60\%$ with no significant variations throughout the day (Fig. 1d). The ~~pancake concentration observed~~ observed pancake concentration diverged from satellite observations (AMSR2) of sea ice concentration (see Fig. 1d), as the AMSR2 concentration includes the interstitial frazil ice, which is intentionally excluded from the image processing (i.e. detection of pancake ice only). Moreover, satellite data are an average over two daily swaths. Due to the intense storm activity and the associated drift of the ice edge ($\approx$100 km Eastward in a day) at that time, this average may not be fully representative of the instantaneous conditions, resulting in underestimation of the encountered ice concentration. In this regard, bridge observations following the Antarctic Sea Ice Processes and Climate protocol (ASPeCt, Worby et al., 2008), indicated a 90–100% concentration of total ice, where pancake ice was the primary ice type with concentration of 50–60% for most of the cruise (de Jong et al., 2018), in agreement with the image processing.

3 Pancake ice shape and floe size distribution

Approximating the floe shape as an ellipse, major (D_1) and a minor (D_2) axes are extracted. It is common practice, however, to define one representative dimension as a characteristic diameter ~~$D = \sqrt{4A/\pi}$~~ $D = \sqrt{4S/\pi}$, by assuming that the pancake is a disk (Toyota et al., 2016)~~.~~ , noting that other metrics are also widely used, e.g. the mean caliper diameter (Rothrock and Thorndike, 1984). Only floes entirely within the field of view are considered for these operations. Detection of small floes with $D < 0.25$ m is prone to error ~~and~~ due to the limited number of pixels of which these floes are comprised and, thus, excluded from the analysis (Toyota et al., 2011). Moreover, a small fraction of large floes ($< 10\%$ of floes larger than 5 m) were artificially welded by the image processing. These floes were also excluded. In total, 4×10^5 individual floes were considered over an equivalent sampled area of ≈ 1.55 km^2, and spanning almost 100 km of non-contiguous marginal ice zone.

Fig. 3a presents a scatter plot of the aspect ratio ($D_1 : D_2$). On average D_1 is $\approx 60\%$ greater than D_2 (slope of a linear fit). ~~It is interesting to note that this~~ This aspect ratio is similar to ~~the~~ one observed for broken ice floes (Toyota et al., 2011). The inset shows the full probability distribution of the ratio D_1/D_2 and indicates that floes elongated such that $D_1/D_2 > 3$ are infrequent. Fig. 3~~b~~ d shows the circularity $C = 4\pi S/P^2$, where P is the floe perimeter (for a circle $C = 1$), which characterises the shape of the floes, noting that other metrics can be used to define the roundness of the floes (Hwang et al., 2017). For floes up to $D \approx$6 m, the average circularity, denoted by the continuous line, is $C \geq 0.75$. Similar values have been reported for much larger broken floes (Lu et al., 2008).

Fig. 3b and 3e display the floe size area distribution as exceedance probability and probability density function respectively. Fig. 3e shows that, in terms of the equivalent diameter (D), 50% of the pancake area is comprised of floes with diameters in the range 2.3–4 m. The mode of the area distribution is 3.1 m (median and mean are ≈ 3.1 m and ≈ 3.2 m respectively), compared to $D_1 = 4$ m and $D_2 = 2.6$ m using the major and the minor axes.

~~In (a), scatter plot of the major and minor axis of the pancake floe with the linear fit (solid orange line). In (b), ice area distribution as a function of the floe diameter. In (c), floe number exceedance probability $N(D)$ as a function of the floe diameter with two power law (solid orange lines) fitted for small ($D < 2.3$ m) and large floes ($D > 4$ m) respectively. In (d), floe number probability density function $n(D)$ as a function of the floe diameter with two power law (solid orange lines) fitted for small ($D < 2.3$ m) and large floes ($D > 4$ m) respectively.~~

Fig. 3c shows the exceedance probability $N(D)$, which exhibits two distinct slopes in the log-log plot, with a smooth transition from mild to steep slopes around the dominant diameter of 3.1 m. The probability density function of the equivalent diameter $n(D)$, shown in Fig. 3~~d~~f, displays a pronounced hump in the transition between, revealing a third regime (2.3 m$<$ $D < 4$ m) around the modal pancake diameter, which is hidden in the exceedance probability~~.~~

~~Assuming, as standard, a power law $N(D) \propto D^{-\alpha}$ as a benchmark and using the maximum likelihood method, we determine $\alpha = \alpha_S = 1.1$ for small floes (~~, where the small- and large-floe regimes are defined as $D < 2.3$ m ~~) and $\alpha = \alpha_L = 9.4$ for large floes (~~and $D > 4$ m ~~). (Note that the maximum recorded diameter was $D = 10.8$ m, and, therefore, the estimation of the scaling exponent for $D > 4$ m is rigorously not applicable, as less than a decade of length scale is available.)Therefore, according to the power-law fit, the large-floe slope is ≈ 8.5 times greater than the small-floe slope.~~ (somewhat arbitrarily).

Small floes ($D < 2.3$ m) constitute the vast majority of the total detected floes ($> 80\%$). In this regime, the mild slope of $N(D)$ may result from a continuous process of floes accretion (from frazil to larger pancakes) regulated predominantly by thermodynamic freezing processes (Roach et al., 2018b). Floes larger than 4 m are detected far less frequently ($< 5\%$ of the total floes), and the steeper slope indicates that their size is most likely governed by different underlying physical mechanisms. Visual examination of the acquired images shows that the majority of the large floes are composed of two or more welded pancakes ~~. The welding processis~~ suggesting that the welding process, promoted by the high concentration of pancakes and the presence of interstitial frazil ice (Roach et al., 2018b)~~.~~, could be the dominant underlying mechanism for the shape of the probability distribution of large floes. Finite size effects are ruled out because the change in slope occurs for $D \approx 4$ m which is considerably smaller than the image footprint.

Assuming, as standard, a power law $N(D) \propto D^{-\alpha}$ as a benchmark and using the maximum likelihood method following Stern et al. (2018), we determine $\alpha = \alpha_S = 1.1$ for small floes ($D < 2.3$ m) and $\alpha = \alpha_L = 9.4$ for large floes ($D > 4$ m). (Note that the maximum recorded diameter was $D = 10.8$ m, and, therefore, the estimation of the scaling exponent is rigorously not applicable in either of the two regimes, as less than a decade of length scales are available.)

The power-law ~~fit is an approximation~~ fits are approximations only, and an objective Kolmogorov–Smirnov goodness-of-fit test (Clauset et al., 2009) reveals that the empirical pancake size distribution does not scale accordingly to a power law in either the small- or large-floe regime, noting ~~that the characteristic diameter itself is a crude (although often useful)metric to quantify floe size.~~ the power law hypothesis is more likely to be rejected when tested over limited diameter ranges (i.e. less than a decade). A close inspection ~~at~~ of the empirical distribution shows that $N(D)$ possesses a slightly concave-down curvature across all the diameter ranges (in a log-log plane)~~and the~~, which is commonly associated with a truncated power law (Stern et al., 2018). The corresponding $n(D)$ displays ~~a~~ an S-shape in the small-floe regime (it shifts from a concave-down to a concave-up curvature at $D \approx 1$ m) in contrast to the hypothesis of a power law behaviour. Deviations from the power law scaling are prominent towards the extremes of the intervals ($D \to 0.25$ m and $D \to 2.3$ m for the small-floe regime; $D \to 4$ m and $D \to 10$ m for the large-floe regime) but become conspicuous only by examining the empirical distribution over limited diameter ranges and probability intervals (i.e. zooming in on Figs. 3~~c–d).~~ c–f). We also note that an increasing $a(D)$ in the small-floe regime (see Figs. 3e) is inconsistent with a power law with $\alpha_S \geq 1$ and, thus, the area distribution confirms that the underlying number distribution is not a power law.

Goodness-of-fit tests also rule out floe size distributions such as the truncated power law (Stern et al., 2018), generalized Pareto (Herman, 2010), and linear combination of Gaussian distribution and power law (Herman et al., 2017). It appears that an accurate approximation of the floe size distribution (in the goodness-of-fit sense) can only be achieved by dropping any a priori assumptions on the functional shape, e.g. by using a nonparametric kernel density estimation (Botev et al., 2010). However, this does not provide any insight on the underlying physical processes responsible for the shape of the empirical distribution.

4 Conclusions

Observations of pancake ice floe sizes during the winter expansion of the Antarctic marginal ice zone were analysed. An automatic floe detection algorithm was used to extract metrics (diameter and area) of the pancake floes, for which the equivalent diameter (~~$D = \sqrt{4A/\pi}$~~ $D = \sqrt{4S/\pi}$) ranged between 0.25–10 m. This allowed a quantitative representation of the pancake size distribution to be discussed.

The floe size distribution displays three distinct regimes, which are visible in the probability density function that, compared to the commonly reported exceedance probability, is more informative. One regime is $D = 2.3$–4 m, centred around the dominant pancake diameter of 3.1 m, which covers half of the total pancake area, and appears as a hump in the probability density function. Two different behaviours ~~qualitatively close to power law scalings~~ are observed for smaller and larger pancakes on a log-log plane. The small-floe regime ($D < 2.3$ m), in which it is conjectured that pancakes are experiencing thermodynamic growth, is characterised by a mild negative slope (in terms of the floe number exceedance and probability density function), while the large-floe regime, in which floes are typically formed by welding (detected from visual analysis), is characterised by a much steeper slope ~~.~~noting that neither of the two regimes conform to a power law scaling.

These results reflect observations collected under storm conditions and, thus, lack generality. Simultaneous measurements of waves, floe size and heat fluxes under a number of different conditions are needed to verify the conjecture that different physical mechanisms (e.g. thermodynamic growth and welding) are responsible for the peculiar shape of the pancake ice floe size distribution.

Code and data availability. The detection algorithm and the acquired images are available upon request to the corresponding author.

Competing interests. The authors declare that they have no conflict of interest.

Acknowledgements. The cruise was funded by the South African National Antarctic Programme through the National Research Foundation. This work was motivated by the Antarctic Circumnavigation Expedition (ACE) and partially funded by the ACE Foundation and Ferring Pharmaceuticals. Support from the Australian Antarctic Science Program (project 4434) is acknowledged. MO was supported by the "Departments of Excellence 2018–2022" Grant awarded by the Italian Ministry of Education, University and Research (MIUR) (L.232/2016). CE was supported under NYUAD Center for global Sea Level Change project G1204. The authors thank Lotfi Aouf at Meteo France for providing reanalysis data and the editor Ted Maksym for useful comments. AA and AT acknowledge support from the Air-Sea-Ice Lab Project. MO acknowledges B GiuliNico for interesting discussions. AA, AT and MO thank LE Fascette for technical support during the cruise.

References

Beitsch, A., Kaleschke, L., and Kern, S.: Investigating high-resolution AMSR2 sea ice concentrations during the February 2013 fracture event in the Beaufort Sea, Remote Sensing, 6, 3841–3856, https://doi.org/10.3390/rs6053841, 2014.

Bennetts, L. G., O'Farrell, S., and Uotila, P.: Brief communication: Impacts of ocean-wave-induced breakup of Antarctic sea ice via thermodynamics in a stand-alone version of the CICE sea-ice model, The Cryosphere, 11, 1035–1040, https://doi.org/10.5194/tc-11-1035-2017, 2017.

Botev, Z. I., Grotowski, J. F., and Kroese, D. P.: Kernel density estimation via diffusion, The annals of Statistics, 38, 2916–2957, 2010.

Clauset, A., Shalizi, C., and Newman, M.: Power-Law Distributions in Empirical Data, SIAM Review, 51, 661–703, https://doi.org/10.1137/070710111, 2009.

de Jong, E., Vichi, M., Mehlmann, C. B., Eayrs, C., De Kock, W., Moldenhauer, M., and Audh, R. R.: Sea Ice conditions within the Antarctic Marginal Ice Zone in WInter 2017, onboard the SA Agulhas II, https://doi.org/10.1594/PANGAEA.885211, 2018.

Dee, D., Uppala, S., Simmons, A., Berrisford, P., Poli, P., Kobayashi, S., Andrae, U., Balmaseda, M., Balsamo, G., Bauer, P., Bechtold, P., Beljaars, A., van de Berg, L., Bidlot, J., Bormann, N., Delsol, C., Dragani, R., Fuentes, M., Geer, A., Haimberger, L., Healy, S., Hersbach, H., Hólm, E., Isaksen, L., Kållberg, P., Köhler, M., Matricardi, M., McNally, A., Monge-Sanz, B., Morcrette, J., Park, B., Peubey, C., de Rosnay, P., C., T., Thépaut, J., and Vitart, F.: The ERA–Interim reanalysis: configuration and performance of the data assimilation system, Quarterly Journal of the Royal Meteorological Society, 137, 553–597, https://doi.org/10.1002/qj.828, 2011.

Gherardi, M. and Lagomarsino, M. C.: Characterizing the size and shape of sea ice floes, Scientific reports, 5, 10 226, 2015.

Herman, A.: Sea-ice floe-size distribution in the context of spontaneous scaling emergence in stochastic systems, Phys. Rev. E, 81, 066 123, https://doi.org/10.1103/PhysRevE.81.066123, 2010.

Herman, A., Evers, K.-U., and Reimer, N.: Floe-size distributions in laboratory ice broken by waves, The Cryosphere Discussions, 2017, 1–20, https://doi.org/10.5194/tc-2017-186, 2017.

Horvat, C. and Tziperman, E.: A prognostic model of the sea-ice floe size and thickness distribution, The Cryosphere, 9, 2119–2134, https://doi.org/10.5194/tc-9-2119-2015, 2015.

Horvat, C. and Tziperman, E.: The evolution of scaling laws in the sea ice floe size distribution, Journal of Geophysical Research: Oceans, 122, 7630–7650, https://doi.org/10.1002/2016JC012573, 2017.

Hwang, B., Wilkinson, J., Maksym, E., Graber, H. C., Schweiger, A., Horvat, C., Perovich, D. K., Arntsen, A. E., Stanton, T. P., Ren, J., et al.: Winter-to-summer transition of Arctic sea ice breakup and floe size distribution in the Beaufort Sea, Elem Sci Anth, 5, https://doi.org/10.1525/elementa.232, 2017.

Kong, T. Y. and Rosenfeld, A.: Topological algorithms for digital image processing, vol. 19, Elsevier, 1996.

Lu, P., Li, Z. J., Zhang, Z. H., and Dong, X. L.: Aerial observations of floe size distribution in the marginal ice zone of summer Prydz Bay, Journal of Geophysical Research: Oceans, 113, https://doi.org/10.1029/2006JC003965, 2008.

Parmiggiani, F., Moctezuma-Flores, M., and Guerrieri, L.: Identifying pancake ice and computing pancake size distribution in aerial photographs, in: Remote Sensing of the Ocean, Sea Ice, Coastal Waters, and Large Water Regions 2017, vol. 10422, International Society for Optics and Photonics, 2017.

Roach, L., Horvat, C., Dean, S., and Bitz, C.: An emergent Sea Ice Floe Size Distribution in a Global Coupled Ocean–Sea Ice Model, Journal of Geophysical Research: Oceans, https://doi.org/10.1029/2017JC013692, 2018a.

Roach, L., Smith, M., and Dean, S.: Quantifying Growth of Pancake Sea Ice Floes Using Images From Drifting Buoys, Journal of Geophysical Research: Oceans, https://doi.org/10.1002/2017JC013693, 2018b.

Rothrock, D. A. and Thorndike, A. S.: Measuring the sea ice floe size distribution, Journal of Geophysical Research: Oceans, 89, 6477–6486, https://doi.org/10.1029/JC089iC04p06477, 1984.

Shen, H. H. and Ackley, S. F.: A one-dimensional model for wave-induced ice-floe collisions, Annals of Glaciology, 15, 87–95, https://doi.org/10.3189/1991AoG15-1-87-95, 1991.

Shen, H. H., Ackley, S. F., and Yuan, Y.: Limiting diameter of pancake ice, Journal of Geophysical Research: Oceans, 109, https://doi.org/10.1029/2003JC002123, 2004.

Steele, M.: Sea ice melting and floe geometry in a simple ice-ocean model, Journal of Geophysical Research: Oceans, 97, 17 729–17 738, https://doi.org/10.1029/92JC01755, 1992.

Steer, A., Worby, A., and Heil, P.: Observed changes in sea-ice floe size distribution during early summer in the western Weddell Sea, Deep Sea Research Part II: Topical Studies in Oceanography, 55, 933 – 942, https://doi.org/10.1016/j.dsr2.2007.12.016, 2008.

Stern, H., Schweiger, A., Zhang, J., and Steele, M.: On reconciling disparate studies of the sea-ice floe size distribution, Elem Sci Anth, 6, https://doi.org/10.1525/elementa.304, 2018.

Toyota, T., Haas, C., and Tamura, T.: Size distribution and shape properties of relatively small sea-ice floes in the Antarctic marginal ice zone in late winter, Deep Sea Research Part II: Topical Studies in Oceanography, 58, 1182 – 1193, https://doi.org/10.1016/j.dsr2.2010.10.034, 2011.

Toyota, T., Kohout, A., and Fraser, A. D.: Formation processes of sea ice floe size distribution in the interior pack and its relationship to the marginal ice zone off East Antarctica, Deep Sea Research Part II: Topical Studies in Oceanography, 131, 28 – 40, https://doi.org/10.1016/j.dsr2.2015.10.003, 2016.

Wadhams, P., Aulicino, G., Parmiggiani, F., Persson, P. O. G., and Holt, B.: Pancake Ice Thickness Mapping in the Beaufort Sea From Wave Dispersion Observed in SAR Imagery, Journal of Geophysical Research: Oceans, https://doi.org/10.1002/2017JC013003, 2018.

Worby, A. P., Geiger, C. A., Paget, M. J., Van Woert, M. L., Ackley, S. F., and DeLiberty, T. L.: Thickness distribution of Antarctic sea ice, Journal of Geophysical Research: Oceans, 113, https://doi.org/10.1029/2007JC004254, 2008.

Zhang, J., Schweiger, A., Steele, M., and Stern, H.: Sea ice floe size distribution in the marginal ice zone: Theory and numerical experiments, Journal of Geophysical Research: Oceans, 120, 3484–3498, https://doi.org/10.1002/2015JC010770, 2015.

Zhang, J., Stern, H., Hwang, B., Schweiger, A., Steele, M., Stark, M., and Graber, H. C.: Modeling the seasonal evolution of the Arctic sea ice floe size distribution, Elem Sci Anth, 4, https://doi.org/10.12952/journal.elementa.000126, 2016.